Biosensors and Bioelectronics 66 (2015) 290–296

Contents lists available at ScienceDirect

Biosensors and Bioelectronics

journal homepage: www.elsevier.com/locate/bios

Real-time and label-free analyte detection in a flow-through mode using immobilized fluorescent aptamer/quantum dots molecular switches

Anastasia Bogomolova *, Matt Aldissi

Smart Polymers Research Corporation, 108 4th Street, Belleair Beach, FL 33786, USA

ARTICLE INFO

Article history:
Received 9 August 2014
Received in revised form
23 October 2014
Accepted 18 November 2014
Available online 20 November 2014

Keywords:
Aptamer
Biosensor
Quantum dots
Real-time
Toxin
Flow-through

ABSTRACT

Inspired by the goal to create a biosensor with designer specificity for real-time detection of unlabeled analytes in a flow-through mode, we designed a miniature flow cell with interchangeable quartz window carrying immobilized aptamer/quantum dot molecular switches as a part of a portable fluorescent setup. The inner surface of the 1.5 mm ID, 12 μl flow cell quartz window has been modified with the aptamer sensing complexes containing highly-fluorescent quantum dots. The aptamer complexes were designed as molecular switches to undergo conformational change and release fluorescent label upon interaction with the flow of the analyte, causing fluorescence decrease. The specificity of the sensor was designed to address the light chain of Botulinum Neurotoxin A and Ricin Toxin A chain, which could be specifically and repeatedly detected in the flow of 60 μl/min with sensitivity comparable to other real-time detection methods. The specifics of quantum dots use as fluorescent labels for continuous monitoring under constant UV illumination were outlined. The possibility for multispecific sensing was explored by testing of bi-specific sensor. This work shows the possibility of surface-bound aptamer sensing for flow-through analyte detection and provides a useful tool to perform surface fluorescent studies in real-time. The flexibility of the described design allows for sensor specificity change through altering the specificity of the aptamer. Future work should address response quantification. The described sensing approach can be adapted to a number of environmental or clinical targets.

1. Introduction

Specific recognition of biomolecules is the essence of all communications in Nature. Biosensors combine the principle of biological recognition with signal transduction, producing measurable and quantifiable output, which can be analyzed. Obtaining a biosensor output in real-time gives an important advantage of providing a rapid response, which is especially relevant for environmental outbreaks and medical emergencies.

Exponential growth of biosensing publications, currently exceeding 4000 research papers annually characterizes high need and numerous applications of biosensors. Real-time biosensors constitute less than 10% of that due to complexity of the task to combine adequate sensitivity with high detection speed. While PCR-based methods are unsurpassed in sensitivity and are used in more than half of the real-time biosensing methods, they can only detect the living matter, possessing the genetic material, which leaves out individual molecules, proteins, toxins, heavy metals and other potential analytes. Contrary to PCR-based methods, biorecognition events with key-lock specificity, such as between antigen and antibody or aptamer and its target can be used to directly detect a wider range of analytes of organic and inorganic nature. Used in conjunction with electrochemical or optical signal output, it can result in a biosensor suitable for point-of-care or field diagnostic.

Stability of DNA aptamers in a wide range of temperature conditions makes them a popular choice over antibodies for a number of biosensing applications. A number of aptamers specific to environmental and food pathogens, including viruses, bacteria, spores, toxins and heavy metals have been used for biosensor development and recently reviewed (Amaya-González et al., 2013; Sekhon et al., 2013; Kiilerich-Pedersen et al., 2013). The aptamers also attract researchers by the possibility of rational design, such as, for example, molecular switches used in biosensors (Plaxco and Soh, 2011; Tang et al., 2014) and smart materials (Mastronardi et al., 2014). Another possibility is detecting an aptamer binding event through nucleic acid amplification (Ma et al., 2012), which

* Corresponding author.
E-mail address: abogomol@hotmail.com (A. Bogomolova).

http://dx.doi.org/10.1016/j.bios.2014.11.034
0956-5663/

efficiently converts detection of non-genetic material into nucleic-acid detection method with all the advantages of down-to-one-molecule sensitivity potential.

The kinetics of aptamer binding allows for real-time monitoring. While real-time aptasensors can have electrochemical (Chang et al., 2014; Zheng et al., 2014) or optical (Yildirim et al., 2012) signal output, they are typically based on folding of the aptamer upon analyte binding, which causes the signal. In case of aptamer beacons, the quencher on a complementary strand can be displaced by an analyte, allowing monitoring of signal accumulation in a matter of seconds (Tuleuova and Revzin, 2010). The aptamers can be also surface-bound and even anchored on cell surface, registering chemical transmitter release in real-time (Tokunaga et al., 2012).

Real-time aptamer-based detection can be performed in a flow-through mode. Thus, a microfluidic electrochemical aptasensor capable of real-time measurement of therapeutic agents in blood in living animals has been recently reported (Ferguson et al., 2013), significantly advancing the sensing capacity to the desirable point-of care diagnostics.

With multiple existing aptamers specific to environmental pollutants (Long et al., 2013), one can expect a development of a family of real-time flow sensors for on-site monitoring. Thus developing a universal platform with interchangeable specificity is highly desirable.

We have been focusing on a modular approach for fluorescent real-time aptasensor, aiming at simplicity and portability. We have previously reported a concept of real-time flow aptasensor using stable quantum dots (QD) fluorescence detection (Bogomolova and Aldissi, 2011). The versatility of QDs has been especially popular for intra-cell and tissue monitoring, as well as for many other biosensing applications. The idea of combining aptamer sensing and quantum dot fluorescence is entering the real-time biosensing field (Yang et al., 2014). With a potential for multispecific detection, QD can also become a useful tool for expansion of existing real-time sensing approaches. Exploring the performance of QDs in a flow sensor format, we have developed a miniature flow aptasensor, suitable for modular assembly, rapid exchange of sensor functionality and multispecific detection.

2. Materials and methods

Commercially available QD Conjugates were used in this study. Semiconductor nanocrystals with CdSe core, encapsulated in ZnS and polymer shells, modified with covalently attached streptavidin, "Qdot® ITK™ Streptavidin Conjugates" (15–20 nm for QD 565-QD705 conjugates, correspondingly) were purchased from Invitrogen Life technologies. Phosphate-buffered saline (PBS) and deionized water were purchased from Invitrogen Life technologies. Ricin Toxin Chain A (RTA) and other chemicals were purchased from Sigma-Aldrich. Botulinum Neurotoxin Type B Light Chain (BoNTA-LC) was purchased from List Biological Laboratories (CA, USA). Custom oligonucleotide synthesis and HPLC purification was performed by Eurofins Genomics (formerly Operon).

Flow Cell components: Quartz tubes (1.5 mm ID, 2.5 mm OD × 7 mm) were custom-cut by Donghai Xuri Lighting Electric Apparatus Co. (China) and (1.5 mm ID, 2.5 mm OD × 6.5 mm) by Polymicro Technologies, Molex Inc. (AZ, USA); silicone tubing was purchased from Altec Products LTD (UK), and custom flow cell body was designed and manufactured by ALine Inc. (CA, USA), Fig. 1.

The portable fluorescent setup included LED 400 nm light source, two fiber optic cables, cuvette holder and miniature USB2000 fiber optic spectrophotometer, all from Ocean Optics (FL, USA) and a variable speed peristaltic pump from Fisher Scientific. The fluorescence spectra and real-time intensity data were recorded using Spectra Suite acquisition software (Ocean Optics) on a laptop computer. (Fig. A1).

2.1. Oligonucleotide probe design

1) AT-Anchor oligonucleotide (used to coat silanized quartz and immobilize the aptamers): 5′-AAAATAAAATAAAATAAAA-TAAAATAAAAT-3′
2) BLC oligonucleotide (aptamer specific to the light chain of botulinum neurotoxin A (Lou et al., 2009) with added 5′ T-rich sequence complementary to AT-anchor for immobilization). Aptamer sequence is shown in bold. Positions of complementary detector oligonucleotides are underlined.
5′-TTTTATTTTATTTTATTTT-CTTGAGTGTCATGG
ACGTTCCGGTCTTGGGCGGGATATTTGTTTGTTTTCTGCCTATGTT-
3′ LC1 LC2 LC3 LC4
3) Detector oligonucleotides (end-biotinylated and partially complementary to BLC aptamer, designed to disrupt possible stem-loop conformations, shown in Fig. A2, appendix A). Complementary portions are shown in bold.
Detector LC1: 5′ biotin-(A_{12})CCATGACACT 3′
Detector LC2: 5′ biotin-(A_{12})ACCGGAACGT 3′

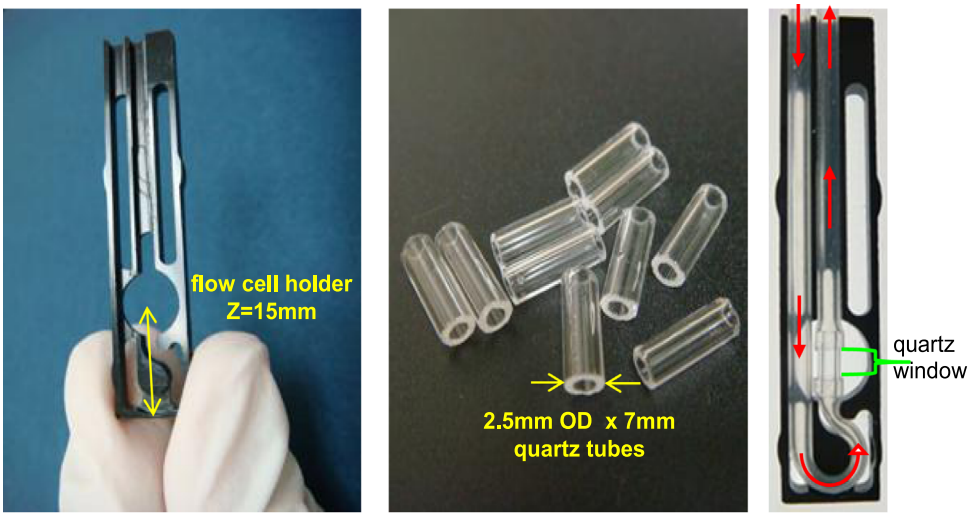

Fig. 1. "Interchangeable Window" flow cell (IWFC). Quartz tube inner volume = 12 μl. The inner surface of quartz tubes is modified with a sensing complex. The tubes are easily interchanged using flexible silicon tubing. IWFC fits diagonally into a cuvette.

Detector LC3: 5′ biotin-(A_{12})ATCCCGCCC 3′
Detector LC4: 5′ biotin-(A_{12})CAGAAAACAAAC 3′

4) RKD oligonucleotide (DNA analog of RNA aptamer, specific to Ricin Toxin Chain A (Kirby et al., 2004), with added 5′ T-rich sequence complementary to AT-anchor for immobilization). Aptamer sequence is shown in bold, positions of complementary detector oligonucleotides are underlined.
5′-TTTTATTTTATTTTATTTTAAAAGGCGAATTCAGGGACGTAGCAATGACTGCC-3′ K1 K2 K3
5) Detector oligonucleotides (end-biotinylated and partially complementary to RKD aptamer, designed to disrupt possible stem-loop conformations, shown in Fig. A3, Appendix A). Complementary portions are shown in bold. Detector K1: 5′ biotin-GCAGGGCTGAATTCGC Detector K2: 5′ biotin-TAACGAACGTCCCCT Detector K3: 5′ biotin-ACTGCCCAGTCATTGC

2.2. Sensing complex preparation

The sensing complex was prepared on the inner surface of custom-cut quartz tubes (1.5 mm ID, 2.5 mm OD × 7 mm).

2.2.1. Immobilization surface preparation

Tube surface cleaning and silanization has been optimized for efficient sensing complex immobilization. The detailed procedure can be found in Appendix B. During the cleaning, the surface was enriched in hydroxyl groups, which was necessary to allow efficient silanization. Silanization was performed using low concentration (0.02%) of Glycidoxy-propyl-3-ethoxy silane (GOPS) in anhydrous ethanol for 16–48 h to avoid multilayer silane formation.

2.2.2. Surface modification

The modification included several consecutive steps (Fig. 2A). The detailed surface modification procedure is described in Appendix B.

1) Anchor oligonucleotide ($A_4T)_6$ was attached through the reaction of aminogroups of nucleobases with the epoxy group of the silane. This attachment also served as an efficient blocking agent by binding available epoxy groups of the silane due to the high concentration during the immobilization (1 mg/ml, or ~0.1 mM concentration)
2) The aptamer/biotinylated detector oligonucleotide complex was pre-annealed in solution at 10 pM concentration and hybridized to the anchor. Alternatively, this step could be done in two consecutive annealing steps as shown in Fig. 2, by hybridizing the aptamer to the anchor, and the biotinylated detector to the aptamer.
3) The quantum dot-streptavidin conjugate was attached to the biotinylated detector at 20–60 nM, completing the fluorescent sensing complex assembly.

The described sensing complex immobilization and assembly method was found preferential to the previously used method through Streptavidin (Bogomolova and Aldissi, 2011), Fig. A4-A, Appendix A). It allowed denser aptamer immobilization (resulting in complexes with higher fluorescence), while simultaneously providing oligonucleotide-blocked surface, which reduced nonspecific binding. The fact that oligonucleotide would get preferentially immobilized on epoxy-silane through the side aminogroups of nucleobases rather than end aminogroup was found experimentally through poor end aminogroup immobilization of an aptamer, which was easily competed by nonspecific Calf Thymus DNA (Fig. A4–B, Appendix A). The efficiency of immobilization and assembly was estimated from comparison of the fluorescence of the resulting complexes with background fluorescence of complexes with missing components, such as aptamer or detector, which signified background nonspecific binding of one of the components.

For bi-specific sensing, two types of the sensing complexes containing a different type of an aptamer, detector and QD/Streptavidin conjugate as a label were immobilized simultaneously on the surface of IWFC tube. Individual sensing complexes were pre-assembled in solution prior to immobilization.

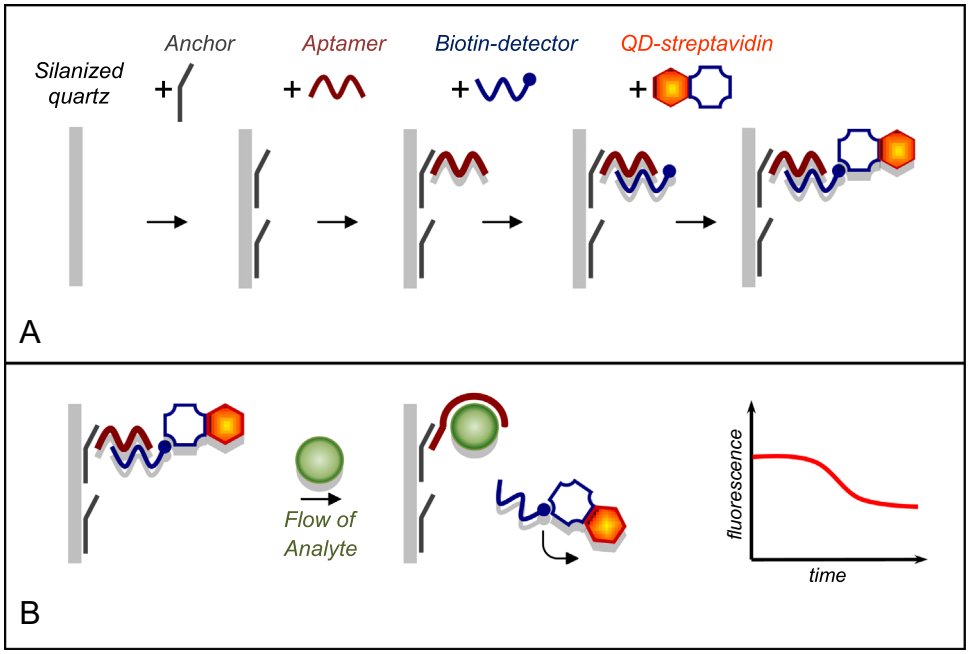

Fig. 2. Sensing complex assembly and detection scheme. (A) Sensing complex is self-assembled on the inner surface of the quartz tube in four steps; (B) The analyte is detected through fluorescence decrease in real-time.

2.3. Flow cell assembly

The modified quartz tube was used as UV-transparent window of the flow cell (see Fig. A5, Appendix A for step-by-step assembly and Appendix B for detailed description). Non-reflective Delrin polymer holder (custom-made by ALine Inc.) was used to hold the silicon tubing providing the flow to the window. (IWFC, Fig. 1). IWFC was inserted diagonally into a fluorescent cuvette and connected to the flow of buffer/analyte.

2.4. Real-time analyte detection

The fluorescent setup is shown in Fig. A1 (appendix A) and the details of the experimental procedure are described in Appendix B. The flow cell was connected to the flow of PBSM buffer and allowed to release weakly-bound quantum dots for 5–10 min. without UV illumination. After the initial wash, the fluorescence was constantly recorded for the whole length of the 2–3 h experiment at a specific wavelength or averaged though a specific range. The baseline was allowed to stabilize for 30 min. prior to connecting to the flow of the analyte. The flow rate was kept constant throughout the measurement, typically 30–60 μl/min.

3. Results and discussion

3.1. Baseline

In order to register a change in a real-time fluorescence measurement, it is necessary to obtain a stable baseline. The fluorescence of quantum dots (QDs) is orders of magnitude brighter and more stable when compared to other fluorophores, but it is not constant. QD fluorescence is a complex phenomenon, with every individual dot blinking with a certain frequency from 200 μs to 100 s (also known as intermittent photoluminescence, (Heuff et al., 2007)), which is apparently affected by their environment. Recording fluorescence at a single QD peak wavelength produced a noisy baseline (Fig. A6-A, Appendix A), while averaging fluorescence over the range of the peak resulted in significant improvement (Fig. A6-B, Appendix A).

However the main challenge of prolonged real-time recording was to account for inherent time-related brightness changes of QDs, with an initial increase in brightness followed by a slow decline (Fig. 3).

The brightness changes presented in Fig. 3 were quite consistent for a variety of used QDs and attachment methods. Whether the QDs were part of the sensing complex, or directly immobilized on the quartz surface did not affect the baseline behavior. Spontaneous detachment of QDs due to the flow was ruled out as the baseline decline was even stronger without the flow (Fig. A7, Appendix A). Gentle flow, at rates up to 100 μl/min for sensing complexes and up to 330 μl/min for directly immobilized QDs actually improved the linear portion of the baseline by slowing down the gradual fluorescence decline, probably due to the increased buffer exchange rate. In the absence of the flow the decline of the baseline accelerated (Fig. A8, Appendix A).

In addition, if the UV illumination was interrupted for 15 min 48 h and resumed, the baseline fluorescence repeated the pattern, with relatively rapid fluorescence increase and gradual decline. As the scale of the baseline changes was somewhat proportional to the density of QD immobilization, (i.e. in the samples with higher fluorescent intensity the changes were slightly more pronounced), we concluded that the baseline behavior is inherent to immobilized populations of QD. We think that mutual self-activation during the first half hour and self-quenching after that are contributing to the shape of the baseline, phenomena that are outside the scope of this study. Relatively high brightness (and thus density) of immobilized QD population was needed to perform real-time measurements and register the analyte binding effect.

While the analyte produced the response (i.e. fluorescence decrease) both during the rising or falling baseline (Fig. A9, Appendix A), it was easier to compare the responses obtained either immediately after baseline achieving the highest value in about half an hour or during the linearly receding portion, as such baseline could be more accurately extrapolated. While the baseline changes recorded over 2.5 h in Fig. 3 are significant, a single analyte detection experiment was typically completed in 20–30 min, and the baseline slope during this time did not exceed one percent of the total fluorescence intensity. The baseline slope was subtracted from the analyte response as outlined in Section 3.2 below.

In addition to the above, we have found other factors affecting the baseline, including buffer composition, ionic strength and oxygenation rate (oxygen sensitivity of QDs was also recently shown by Ziółczyk et al., 2014). We have also noticed that prolonged exposure of immobilized QDs to UV and flow (5–6 h) resulted in a blue shift of the fluorescence peak, possibly due to a partial dissolution of ZnS shell from the CdSe core of the quantum dots, resulting in size decrease (Fig. A10, Appendix A). Although a typical set of experiments required 2–3 h of constant UV illumination of QDs and the peak shift was not as pronounced, averaging the fluorescence over the whole range of the peak (630–680 nm for QD650) allowed to decrease the effect of the blue shift, which would otherwise affect the fluorescence value if recorded at the peak wavelength. Taking the above factors into account prior to analyte detection, real-time recording was performed with the fluorescence averaged over the range of the QD peak, the baseline was allowed to stabilize for 30–35 min (Fig. 3), and possible variables in buffer composition, flow and oxygenation rates were minimized during the analyte exposure.

3.2. Measuring analyte response

After baseline stabilization, the immobilized sensing complex was exposed to the flow of the analyte solution for 10–15 min (scheme Fig. 2B). Interaction of the analyte with the specific

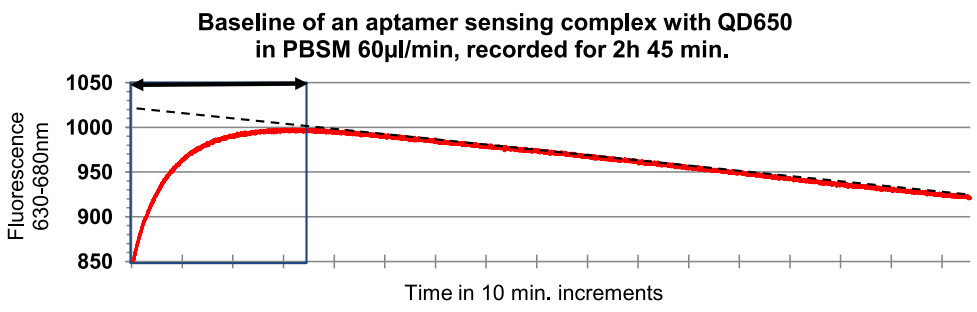

Fig. 3. QD Baseline. Inherent time-related changes in immobilized QD650 fluorescence recorded under flow and constant illumination for 2 h 45 min.

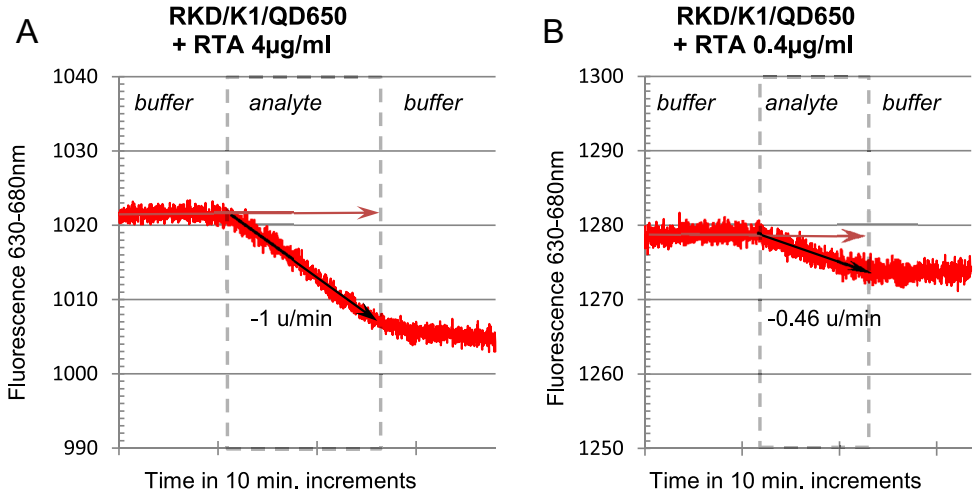

Fig. 4. Measuring analyte response. IWFC with RTA-specific sensing complexes, labeled with QD (650 nm)/Steptavidin conjugate were stabilized in the flow of PBSM 30 μl/min and exposed to 4 μg/ml (A) or 0.4 μg/ml (B) of RTA for 10–15 min.

aptamer caused dissociation of the detector oligonucleotide carrying QD, which was noticeable as fluorescence decrease in real-time, as shown in Fig. 4.

Here fluorescence decrease of a QD-containing RTA-specific sensing complex, RKD/K1/QD650 is caused by the exposure to the specific analyte, RTA. While the original RTA-specific aptamer was selected in RNA form (Kirby et al., 2004), we have compared the predicted secondary structures of the RNA aptamer and its DNA analog, which appeared to be identical (Fig. A3, Appendix A), and tested functionality of the analog DNA aptamer, "RKD". DNA oligonucleotides possess higher stability compared to RNA and are easier to synthesize and handle. To find a responsive sensing complex, we have tested several biotinylated "detector oligonucleotides", with partial complementarity to the aptamer. Detector oligonucleotides were designed to disrupt possible stem-loop conformations of the aptamer. In addition to the complementary portion, the detector oligonucleotides contained non-complementary portion and a biotin on 5′ end to bind streptavidin-QD conjugate during the complex assembly (Fig. 2). Immobilized aptamer with one of the annealed detectors, carrying QD label, would be stable in the flow of the buffer, but release the detector oligonucleotide in the presence of the specific analyte due to the conformational change in the aptamer. DNA aptamer "RKD" was functional in our setup, and the analyte response was visually concentration-dependent (Fig. 4A, B).

To compare analyte-related fluorescence decrease we have calculated fluorescence decrease rate in fluorescence units per minute. Thus, in the above example, RTA at 4 μg/ml (or 125 nM concentration) resulted in a response of [−1 u/min], while ten time lower concentration of RTA was registered as fluorescence decrease with the rate of [−0.46 u/min]. The decrease rate was calculated from the graph by using the linear portion of the response obtained during the analyte exposure.

Comparing responses during the receding baseline required baseline subtraction. To account for the baseline slope during the exposure to analyte, we calculated the rate of the baseline slope by using a linear baseline portion for 10 min prior to the analyte exposure. This rate was subtracted from the rate of the fluorescence decrease, caused by the analyte binding. Thus, in Fig. 5A, the baseline is receding at a rate of [−0.2 u/min], while the exposure to the analyte is causing a decrease of [−2.8 u/min]. To account for the baseline slope, we subtracted the baseline slope rate from the response rate to obtain a normalized rate of [−2.6 u/min]. Obviously, the baseline slope was interfering with measuring the analyte response at lower concentrations.

Out of three detector oligonucleotides tested with RKD DNA aptamer, only K1 formed a responsive complex when exposed to RTA. The other two complexes did not react to RTA. Nonresponsive complex RKD/K2/QD650 is shown in Fig. 5B, also serving as a negative control which shows that RTA by itself is not responsible for fluorescence decrease of QDs. The sensing complex RKD/K1/QD650 was relatively stable and allowed repetitive and next-day detection (Fig. A11-A, A12-B, Appendix A). The presence of the aptamer was essential for the fluorescence decrease, as the complex lacking the aptamer showed no response to RTA (Fig. A11-B). The response to RTA was also specific as BSA produced no response in RKD/K1 complex (Fig. A11-C).

RKD/K1 complex was responsive to RTA in the range of 0.2–16 μg/ml, or 6–500 nM/L. The limit of detection (LOD) was defined by the noise of the baseline and the baseline slope (Fig. A12, Appendix A). Although the response showed concentration-dependent tendencies (Fig. A13), it was strongly affected by surface depletion during repetitive analyte exposures and initial density of the sensing complex, thus variability of the responses remained too high to allow quantification. While the obtained detection limit is 1–2 orders of magnitude higher compared to other Ricin or RTA detection methods which take 1–24 h, summarized by (Pauly et al., 2012), it is comparable to the sensitivity obtained with real-time optical multichannel immunosensor (Bhatta et al., 2011).

Because the specificity of the flow sensor is determined by the specificity of the aptamer, by changing the aptamer sensing complex on the IWFC one can change the specificity. Thus, by using Botulinum-specific aptamer complex we could detect BoNTA-LC at low nanomolar concentrations (Fig. A14, Appendix A). As the aptamer to BoNTA (Lou et al., 2009) had several possible predicted structures (Fig. A2 Appendix A), four possible detector oligonucleotides were tested to find a responsive complex. Two complexes, BLC/LC1 and BLC/LC3 were not responsive to the analyte, while the other two, BLC/LC2 and BLC/LC4 were responsive, with BLC/LC4 being more sensitive, Fig. A14, Appendix A). There is a fine line between designing a sensitive complex and making it too unstable in the flow, and it often lies within one extra complementary nucleotide pair between the detector and the aptamer. While rational design is helpful to select a complementary portion of the detector with the designed T_m, the functional testing is achieved through experimenting with the analyte. In other words, less stable complexes would be more responsive, but it would be harder to achieve a stable baseline with it.

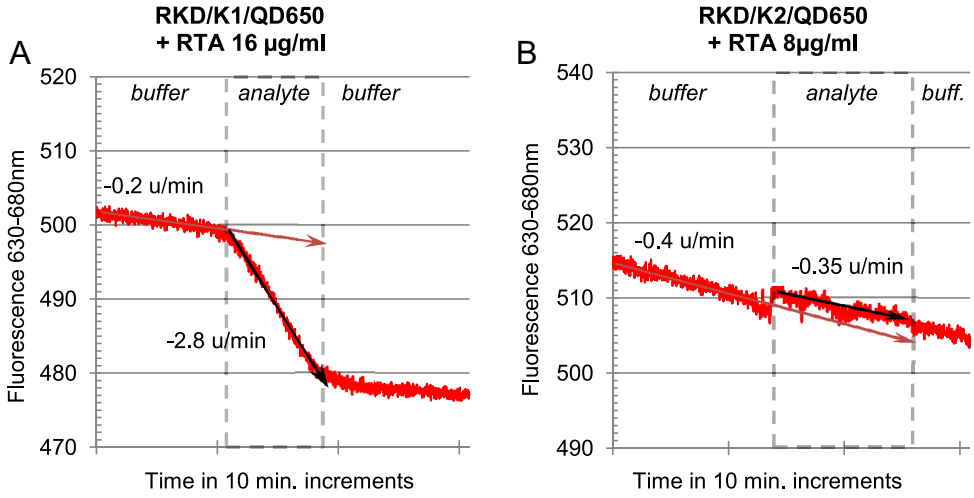

Fig. 5. Measuring analyte response with receding baseline. IWFCs with two different RTA-specific sensing complexes, labeled with QD (650 nm)/Steptavidin conjugates were stabilized in the flow of PBSM 30 µl/min and exposed to the flow of RTA for 10–15 min. (A) RKD/K1 was responding to 16 µg/ml of RTA; (B) RKD/K2 was not responding to 8 µg/ml of RTA. The rates of the baseline slope and the fluorescent decrease resulting from the analyte exposure were calculated in units per minute by linearizing the baseline and the response over 10 min. The baseline slope rate was subtracted from the response rate to obtain normalized response.

3.3. Repetitive analyte detection

We have previously noticed surface depletion phenomena during prolonged exposure to the flow of analyte using ATP-specific aptamer (Bogomolova and Aldissi, 2011). In our current work, we have noticed that while repetitive detection was possible, the signal was decreasing. We took a closer look at surface depletion using eight rounds of exposure of RKD/K1/QD650 complex to a high concentration of RTA (Fig. A15, Appendix A). We have noticed that depleting the surface of the sensing complex does not have a linear effect on the sensor response. Instead, the first two exposures to RTA resulted in high responses, and the next six exposures produced smaller and very comparable responses. Interestingly, while during the last six responses the slope of the baseline changed, the rate of fluorescence decrease during the response remained practically the same, which means that the slope of the baseline is hardly contributing to the fluorescence decrease during the analyte exposure at higher concentrations of the analyte. We hypothesize that optimizing further the density of the sensing complexes on the sensing surface could improve reproducibility of the sensor response.

3.4. Towards multispecific sensing

The fluorescence wavelength of quantum dots depends on their size. To approach the possibility of multispecific analyte detection, one would need to use multiple quantum dots as labels. QD-streptavidin conjugates, in a combination with different aptamers offer a convenient possibility to combine different sensing complexes on one surface. To explore it, first we compared the behavior of different quantum dots in our sensing approach. We have noticed right away that the fluorescence intensity of sensing complexes prepared with different QDs varies significantly, which was related to the difference in fluorescence intensity of different sizes of quantum dots-streptavidin conjugates in solution (Fig. A16, Appendix A). Further testing of the functionality of the sensing complexes showed that, contrary to our expectation, smaller QDs did not perform better when incorporated into sensing complexes. We have noticed that complexes prepared with smaller QD585 and QD605 responded to RTA with a time delay, which was not appropriate for our real-time application. Complexes with bulkier QD655 and QD705 responded immediately upon exposure to RTA (Fig. A17, Appendix A). A possible explanation is that the bulkier QDs contribute to complex destabilization in the flow, thus improving its reactivity to the analyte.

We have used QD 655 and QD705 to test the possibility of a bi-specific sensor. The sensing surface of the quartz tube was modified with two types of sensing complexes with two different specificities: RKD/K1/QD655, specific to RTA, and BLC/LC4/QD705, specific to BoNTA-LC. The complexes were pre-annealed and assembled in solution and immobilized on anchor-modified surface in equimolar ratio. To perform real-time measurement, two channels, corresponding to the fluorescence ranges of QDs were recorded simultaneously. Due to the lower intrinsic fluorescence of QD705, one of the complexes showed lower fluorescence. After stabilization, the bi-specific sensor was exposed to RTA (Fig. A18, Appendix A). RTA-specific complex (RKD/K1/QD655) showed specific fluorescence response to RTA. The nonspecific signal, obtained in a simultaneous fluorescence recording of sensing complex with irrelevant specificity, was low. The scale of the specific response exceeded the response presented in Fig. A13, Appendix A, which might means that immobilizing two different sensing complexes on the same surface did not result in sensitivity decrease.

3.5. Using quantum dots for real-time measurements

We have shown that QDs can provide a useful tool for real-time flow sensing using aptamer molecular switches. There is a number of advantages when using QDs as labels for real-time detection: (a) bright fluorescence of QDs allows constant UV illumination and measurement for hours at a time; (b) commercial availability of QDs with different fluorescence and their streptavidin conjugates offers a variety of possibilities for sensing configurations; (c) physical stability of QDs and their conjugates allows extended detection times and possible storage of sensing complexes. However, several peculiar features of QDs can result in significant drawbacks if not taken into account: (a) the inherent changes in fluorescence intensity of QDs under constant illumination have to be taken into account when measuring the analyte response; (b) the fluorescence of QDs can be affected by their environment, defined by a variety of experimental conditions, such as immobilization density, flow rate, buffer composition and oxygenation rate; (c) the size of QDs is comparable with the size of biological molecules and can become a variable factor when different sizes of QDs are used. Nevertheless, in our experience the

advantages of QDs for real-time flow detection outweighed the drawbacks, and we could successfully incorporate them in an aptamer-based molecular switch sensor, which proved to be functional in real-time.

4. Conclusions

We have designed and tested a portable real-time prototype sensor suitable for fluorescent detection of label-free analytes in flow-through conditions. The miniature flow cell contained interchangeable quartz window with 12 μl internal volume. The surface of the window has been modified with specifically designed aptamer sensing complexes containing highly-fluorescent quantum dots. Detection of the two model protein substrates, light chain of Botulinum Neurotoxin A and Ricin Toxin A chain has been demonstrated. While repetitive analyte detection was possible, the sensing surface depletion caused the response decrease with increased number of detections. The specificity of the sensing responses has been characterized and the guidelines for the use of quantum dots for real-time detection in the flow mode have been developed. The possibility of multispecific detection has been investigated through the assembly and testing of a bi-specific sensor. Flexibility of the sensor design allows for specificity modification to address other analytes through re-designing the aptamer sensing complexes. Further optimization should address standardization of sensing complex immobilization density to decrease response variability and improve baseline stabilization.

Acknowledgments

This work was funded by the US Environmental Protection Agency (EPA), Contract No. EP-D-11-065. The authors are grateful to Dr. E. Komarova and Dr. L. Levine for technical discussions.

Appendix A. Supplementary material

Supplementary data associated with this article can be found in the online version at doi: http://dx.doi.org/10.1016/j.bios.2014.11.034.

References

Amaya-González, S., de-los-Santos-Alvarez, N., Miranda-Ordieres, A.J., Lobo-Castañón, M.J., 2013. Sensors 13, 16292–16311.
Bhatta, D., Michel, A.A., Marti Villalba, M., Emmerson, G.D., Sparrow, I.J., Perkins, E. A., McDonnell, M.B., Ely, R.W., Cartwright, G.A., 2011. Biosens Bioelectron. 30, 78–86.
Bogomolova, A., Aldissi, M., 2011. Biosens. Bioelectron. 26, 4099–4103.
Chang, Y., Chai, Y., Xie, S., Yuan, Y., Zhang, J., Yuan, R., 2014. Analyst 139, 4264–4269.
Ferguson, B.S., Hoggarth, D.A., Maliniak, D., Ploense, K., White, R.J., Woodward, N., Hsieh, K., Bonham, A.J., Eisenstein, M., Kippin, T.E., Plaxco, K.W., Soh, H.T., 2013. Sci. Transl. Med. 5 (213), 213ra165, 10.1126/scitranslmed.3007095.
Heuff, R.F., Swift, J.L., Cramb, D.T., 2007. Phys. Chem. Chem. Phys. 9, 1870–1880.
Kiilerich-Pedersen, K., Daprà, J., Cherré, S., Rozlosnik, N., 2013. Biosens. Bioelectron. 49, 374–379.
Kirby, R., Cho, E.J., Gehrke, B., Bayer, T., Park, Y.S., Neikirk, D.P., McDevitt, J.T., Ellington, A.D., 2004. Anal. Chem. 76, 4066–4075.
Long, F., Zhu, A., Shi, H., 2013. Sensors 13, 13928–13948.
Lou, X., Qian, J., Xiao, Y., Viel, L., Gerdon, A.E., Lagally, E.T., Atzberger, P., Tarasow, T. M., Heeger, A.J., Soh, H.T., 2009. Proc. Natl. Acad. Sci. USA. 106, 2989–2994.
Ma, C., Zhao, C., Ge, Y., Shi, C., 2012. Clin. Chem. 58, 384–390.
Mastronardi, E., Foster, A., Zhang, X., DeRosa, M.C., 2014. Sensors 14, 3156–3171.
Pauly, D., Worbs, S., Kirchner, S., Shatohina, O., Dorner, M.B., Dorner, B.G., 2012. PLoS One 7, e35360.
Plaxco, K.W., Soh, H.T., 2011. Trends Biotechnol. 29, 1–5.
Sekhon, S.S., Kim, S.G., Lee, S.H., Jang, A., Min, J., Ahn, J.Y., Kim, Y.H., 2013. Mol. Cel. Toxicol. 9, 311–317.
Tang, Y., Ge, B., Sen, D., Yu, H.Z., 2014. Chem. Soc. Rev. 43, 518–529.
Tokunaga, T., Namiki, S., Yamada, K., Imaishi, T., Nonaka, H., Hirose, K., Sando, S., 2012. J. Am. Chem. Soc. 134, 9561–9564.
Tuleuova, N., Revzin, A., 2010. Cell. Mol. Bioeng 3, 337–344.
Yang, M., Jiang, B., Xie, J., Xiang, Y., Yuan, R., Chai, Y., 2014. Talanta 125, 45–50.
Yildirim, N., Long, F., Gao, C., He, M., Shi, H.C., Gu, A.Z., 2012. Environ. Sci. Technol. 46, 3288–3294.
Zheng, Y., Chai, Y., Yuan, Y., Yuan, R., 2014. Anal. Chim. Acta. 834, 45–50.
Ziółczyk, P., Kur-Kowalska, K., Przybyt, M., Miller, E., 2014. Spectrochim. Acta A Mol. Biomol. Spectrosc 126, 28–35.